MICROMECHANICAL SIMULATION OF FRACTURE IN POLYMER MATRIX COMPOSITE LAMINATE PLIES

T. D. Breitzman[a*], D. H. Mollenhauer[a], E. V. Iarve[a,b], K. H. Hoos[a,b], E. Zhou[a,b]

[a]*Air Force Research Laboratory, Wright-Patterson Air Force Base, USA*
[b]*University of Dayton Research Institute, Dayton, OH USA*
**Timothy.Breitzman.1@us.af.mil*

Keywords: Fracture, Strength, Multiscale

Abstract
The fracture properties of a unidirectional polymer matrix composite are explored by an a priori calculation of a minimal energy fracture surface separating the microstructure model into two pieces. Subsequent simulations are performed using a regularized version of the extended finite element method in conjunction with the minimal energy fracture surface to derive strength and fracture properties for the microstructure. The resulting properties are compared to results of simulations using different crack paths within the microstructure and reduced interface properties.

1. Introduction

Qualification of material systems and certification of structures for use in aerospace or other applications are rigorous processes used to ensure safety of operation. These processes currently involve a great deal of empirical testing to populate property and performance databases. The amount of testing required is typically time consuming and can be very expensive and thus restricts the utilization of new material and design solutions. Rather, previously qualified materials are used to minimize cost and development time. In order to move past this paradigm, a multiscale simulation approach to offset a portion of the empirical testing is attractive. The focus of this contribution is modeling damage at the microstructure scale to derive properties for the lamina scale.

There are a few main methods by which mechanical damage at the microstructure scale of a composite is typically represented. Particulate, non-continuum approaches such as peridynamics [1] are being employed increasingly often due in part to the imbedded natural framework for fracture simulations. The continuum damage mechanics (CDM) approach [2, 3] operates under the assumption that the effect of damage at finer length scales is a degradation of the local stiffness at the coarser scale. This approach is particularly attractive in a composite microstructure in which the stress field is far from uniform due to the reinforcements, voids, etc. However, as seen in [4], property degradation on the ply level of analysis leads to nonphysical results for local stresses in the damage area and difficulties of damage mode interaction modeling. To address this issue, the Discrete Damage Modeling (DDM) was proposed based on extended finite element method (XFEM) ideas [5] to model discrete cracks of various orientations independent of the mesh.

Multiscale analysis within DDM framework can be accomplished in a fully coupled and simply coupled scale analysis (SCSA) settings, with the simply coupled methods being especially attractive for practical applications. SCSA is an extension of the work [6] where stiffness homogenization and micro level stress bounds estimates where established for pre-stressed composites including regions with nonperiodic microstructure. The proposed extension requires computation of homogenized strength and fracture toughness properties, which are considered below. A direct simulation of failure progression on the micro level is generally required to accomplish this objective. In the present work, we explore a simplified approach, where a minimal energy crack path definition method is proposed in combination with mesh-independent crack (MIC) modeling for micro level failure simulation. The MICs are modeled by using regularized XFEM (rX-FEM) formulation of Iarve [7]. The resulting simulation of the microstructure is then used to predict lamina scale strength and mode-I fracture toughness and compared to experimental data.

2. Methodology

This section discusses how the minimal energy fracture surface is determined and then used in the fracture simulations to derive the strength and fracture properties compared in the results section.

2.1 Determination of the Minimal Energy Fracture Surface

The method described in this section is implemented and works in 3D, but we will use a 2D example to fix ideas. Consider the 2D slice of the composite microstructure pictured in Figure 1. The black area represents the matrix phase and the white areas represent the fiber phase. The goal is to determine a minimal energy fracture surface, or path, through this microstructure. If a discretization of the fiber boundaries is taken so the fibers are represented as polygonal objects, then the *shortest path with obstacles problem* is readily solved by constructing a visibility graph [8] followed by a shortest path algorithm such as the A* algorithm [9] or Dijkstra's algorithm [10].

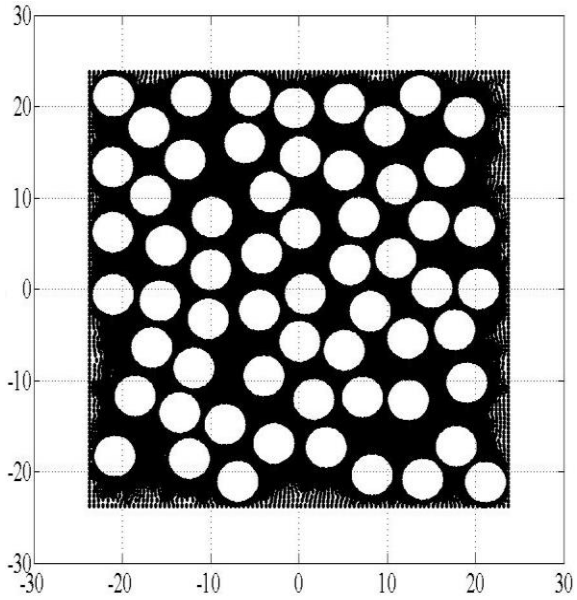

Figure 1. 2D Composite Microstructure Slice with 60 Fibers (scale in μm)

Simply finding the shortest path would result in a path proceeding directly through a fiber or, if we render the fibers impassible, a shortest path around the fibers as in the *shortest path with obstacles problem* referenced above. In our case, we are interested in the *minimal energy path problem*, which we define to be the cleaving path connecting opposite sides of the microstructure having smallest fracture energy. This is not necessarily the shortest path. In fact, the two only coincide when all material and interface fracture properties are equal or a straight line path exists through the weakest material in the system. Thus, the fracture energy of each material and each interface must be accounted for within our framework.

The method by which we determine the minimal energy path is to 1) Discretize the fibers, interfaces, and matrix phases, 2) Create an undirected, weighted graph of the discretized nodes, and 3) Use a graph search algorithm to compute a minimal energy cleaving path on the weighted graph. The discretization of the space can be performed in any manner, except to note that the nodes of the discretization become vertices in the graph. Thus, the density of the nodes is, in general, proportional to the total energy error measured from the global minimum energy path.

We will assume that our crack is only allowed to crack in straight line segments originating at one vertex and terminating at a second, distinct vertex. Thus each edge of the graph represents a possible path the crack could take. Once the vertices are known, the creation of the graph is essentially the determination of the edges of the graph and the assigning of a "weight" or energy, to traverse the edge. We define the weight of the edge to be the fracture toughness multiplied by the distance between the vertices. The fracture toughness for each edge is defined by the appropriate material constant (fiber, matrix, or interface). We consider an edge to exist between two vertices if the distance between the vertices is less than a cut-off radius and either the points are in the same material phase or one vertex is in the interface (see Figure 2). Thus, a crack cannot directly move from the matrix phase to the fiber phase without passing through a vertex on the interface.

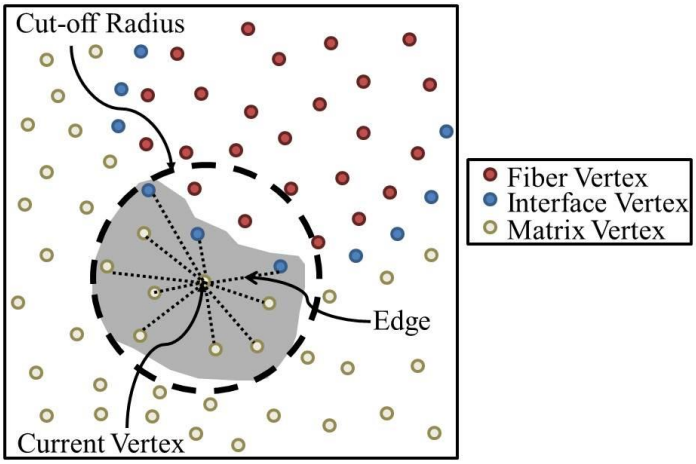

Figure 2. Edge Determination for the Graph

Additionally, we have a visibility requirement so that matrix edges and interface edges cannot pass through a different material phase (see Figure 3).

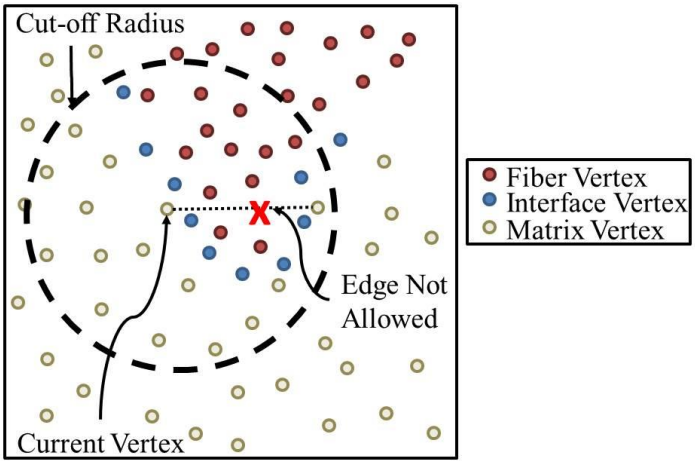

Figure 3. Visibility Restriction on Edges of the Graph

Finally, we supply the weighted graph and an initiation point to the search algorithm to determine the minimum energy path from the initiation point to the goal surface(s). The initiation point may lie on either the interior or exterior of the microstructure, and the crack can be required to fulfill periodicity conditions on the exterior surfaces of the microstructure.

2.2 Calculation of Strength and Fracture Toughness of the Microstructure

The microstructure model undergoes a monotonic loading to failure (two-piece separation). For a microstructure of size $L_{x_1} \times L_{x_2} \times L_{x_3}$ having the x_1 axis being parallel to the axial direction of the fibers, the boundary conditions on the model are monotonic displacement loading on the $x_2 = 0$ and $x_2 = L_{x_2}$ surfaces, $u_{x_1} = 0$ on the $x_1 = 0$ and $x_1 = L_{x_1}$ surfaces, $u_{x_3} = 0$ on the $x_3 = 0$ surface, and traction-free on the $x_3 = L_{x_3}$ surface. The simulation of the progressive damage in the microstructure proceeds by using the minimal energy crack path to define a MIC using the regularized XFEM method described in [7]. Fiber-matrix disbonding is performed in conjunction with the MICs by the surface cohesive law described in [11].

The calculation of the strength and fracture toughness is based on the relationship between the traction and the extension due to damage. The traction – displacement gap relationship, $(T(\Delta u))$, is calculated from the load-displacement curve according to (1)

$$T(\Delta u) = \begin{cases} T = \langle\sigma\rangle_{22}\left(u_{x_2}\right) \\ \Delta u = u_{x_2} - L_{x_2}\left[\left(\overline{S}\langle\sigma\rangle\right)_{22} + \varepsilon_{thermal}\right] \end{cases}, \tag{1}$$

where $\langle\sigma\rangle$ is the volume average stress tensor, Δu is the displacement gap, $\overline{S}$ is the volume average compliance tensor, and $\varepsilon_{thermal}$ is the inelastic strain due to mismatch in thermal expansion coefficients. The displacement gap is thus the difference between the total applied displacement and the elastic displacement resulting from the traction at the current load step (i.e. the displacement due to damage). The transverse strength (σ_T) and mode-I fracture toughness (G_{Ic}) are calculated from the traction – displacement gap relationship as in [12] according to equations (2) and (3).

$$\sigma_T = \max_{\Delta u \in \mathbb{R}_+} \left(T(\Delta u)\right) \tag{2}$$

$$G_{Ic} = \int_{\mathbb{R}_+} T(\Delta u) d(\Delta u) \tag{3}$$

For simplicity, $\varepsilon_{thermal}$ was taken to be zero in all cases in this paper. For reference, the constituent material properties used for simulations and comparison are summarized in Table 1 [13]. It should be noted that the composite properties listed in Table 1 are for a 60% fiber volume fraction, while the composite microstructure used in this paper is only 52% fiber.

	IM7 Fiber	**5250-4 Matrix**	**Composite**
E_{11} (GPa)	276	3.45	167
E_{22}, E_{33} (GPa)	27.6		11.0
ν_{12}, ν_{13}	0.3	0.35	0.32
ν_{23}	0.8		0.51
G_{12}, G_{13} (GPa)	138	1.28	5.33
G_{23} (GPa)	7.67		2.72
α_{11} (/°C)	-0.0360×10^{-6}	46.8×10^{-6}	0.372×10^{-6}
α_{22}, α_{33} (/°C)	5.04×10^{-6}		24.3×10^{-6}
Trans. Stren. (MPa)		77.0	66.0
G_C or G_{Ic} (N/m)		177.0	225.0

Table 1. Constituent and Composite Material Properties

Results

Four initiation points were picked inside the microstructure based on the largest values of failure criteria obtained from the elastic solution. Two crack paths were generated through each initiation point using the minimal energy crack path procedure described above. One path for each initiation point was generated using equal matrix fracture toughness and fiber/matrix interface fracture toughness, and the other was generated using a 20% reduction in the interface fracture toughness (interface strength was not changed). Table 2 summarizes the naming scheme, properties, and crack length for each fracture surface, and Figure 4 shows the microstructure, paths, and initiation points.

Path Name	**Initiation Point (μm)**	**$G_{c_{Int}}$ (N/m)**	**Crack Length (μm)**
P00	(0.00, -2.04, 5.30)	177.0	48.86
P00r	(0.00, -2.04, 5.30)	141.6	49.71
P01	(0.00, 17.30, 7.21)	177.0	49.34
P01r	(0.00, 17.30, 7.21)	141.6	50.96
P02	(0.00, 2.65, -6.09)	177.0	48.16
P02r	(0.00, 2.65, -6.09)	141.6	50.32
P03	(0.00, -18.35, -0.86)	177.0	49.97
P03r	(0.00, -18.35, -0.86)	141.6	50.51

Table 2: Fracture Surface Length for Four Initiation Points and Varying Interface Fracture Energy

As expected, the paths through each initiation point are very similar except for the preference of interfacial fracture when the fiber/matrix fracture energy was decreased. To further study the effect of the path and interfacial fracture toughness on the ply level transverse strength and mode I fracture toughness, both the matrix fracture toughness value and the 20% reduction were applied to all crack paths (in separate runs). Thus, 16 total progressive damage simulations were completed, with the ply level strength and fracture toughness predictions summarized in Table 3.

Path Name	$G_{C_{int}}$ (N/m)	Crack Length (μm)	G_{Ic} (N/m)	σ_T (MPa)
P00	177.0	48.86	224.1	102.5
P00	141.6	48.86	205.5	102.4
P00r	177.0	49.71	250.3	106.5
P00r	141.6	49.71	216.3	105.9
P01	177.0	49.34	237.9	103.3
P01	141.6	49.34	225.9	103.2
P01r	177.0	50.96	237.4	106.4
P01r	141.6	50.96	213.1	106.3
P02	177.0	48.16	236.4	100.8
P02	141.6	48.16	226.9	100.7
P02r	177.0	50.32	232.3	106.3
P02r	141.6	50.32	208.5	106.3
P03	177.0	49.97	271.4	100.5
P03	141.6	49.97	247.5	100.4
P03r	177.0	50.51	235.0	106.4
P03r	141.6	50.51	209.7	106.3

Table 3: Mode-I Fracture Toughness and Transverse Strength Results

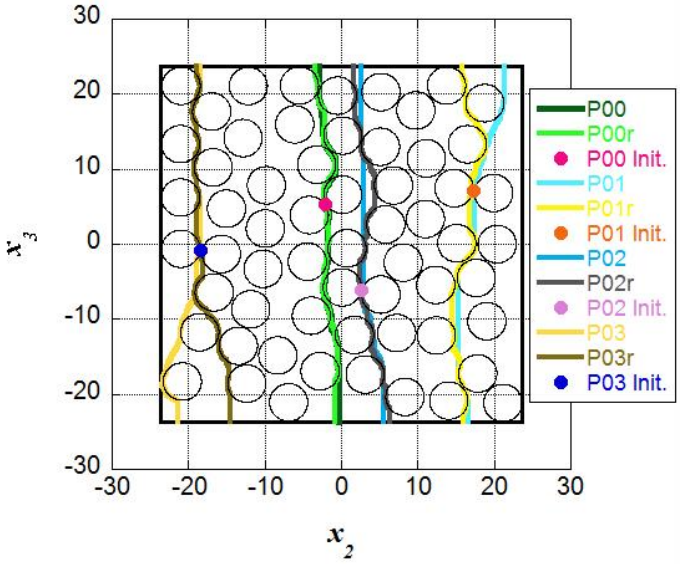

Figure 4: Crack Paths Generated Using the Minimal Energy Method

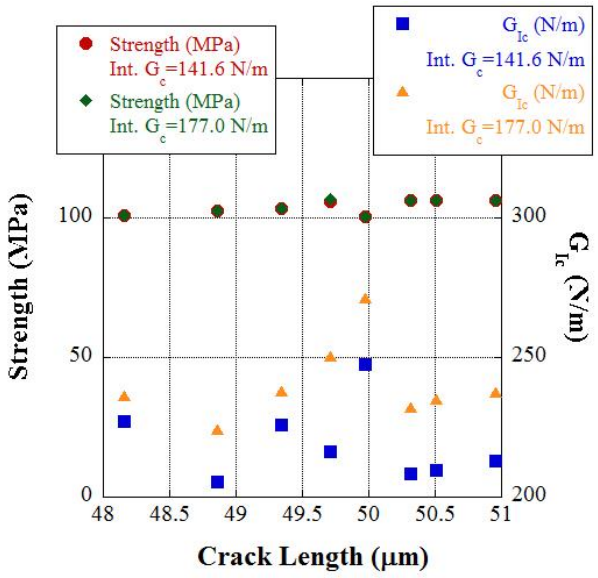

Figure 5: Strength and Fracture Toughness by Crack Length

Conclusions

As expected, the simulations with reduced interfacial fracture toughness predicted a systematically lower ply level mode-I fracture toughness. A 20% reduction in the interfacial fracture energy resulted in a decrease of approximately 10% in the ply level mode-I fracture toughness. The ply level mode-I fracture toughness appears to be somewhat sensitive to the crack length, however, as crack length scatter of 6% produced a 20% scatter in the predicted fracture toughness. It is doubtful that a direct relationship between crack length and fracture toughness exists, as can be seen in Figure 5.

The interfacial fracture toughness had no noticeable effect on the predicted transverse strength (see Table 3 and FIGURE 5). The 6% scatter of crack length produced a strength scatter of 6%, but the strengths predicted in this study are so large (150% of the experimentally measured value) that the agreement in scatter may just be coincidence.

Prediction of mode-I fracture toughness appears to be captured well by this method. Strength requires further examination and may require varying the strength of the interface and/or the inclusion of defects such as porosity.

Acknowledgements

Funding for this work was provided by the Air Force Office of Scientific Research through projects 12RX13COR and 13RX03COR.

References

[1] E. Oterkus and E. Madenci, "Peridynamics of fiber-reinforced composite materials," *Journal of Materials and Structures*, vol. 7, no. 1, pp. 45-84, 2012.

[2] R. Talreja, "Damage Develoment in Composites: Mechanism and Modeling," *Journal of Strain Analysis*, vol. 24, pp. 215-222, 1989.

[3] S. Swaminathan and S. Ghosh, "Statistical Equivalent Representative Volume Elements for Unidirectional Composite Microstructures: Part II - With Interfacial Debonding," *Journal of Composite Materials*, vol. 40, no. 7, pp. 583-604, 2006.

[4] E. V. Iarve, D. H. Mollenhauer and R. Kim, "Theoretical and experimental investigation of stress redistribution in open hole composite laminates due to damage accumulation," *Composites: Part A,* vol. 36, pp. 163-171, 2005.

[5] N. Moes, J. Dolbow and T. Belytshko, "A Finite Element Method for Crack Growth Without Remeshing," *International Journal for Numerical Methods in Engineering,* vol. 46, pp. 131-150, 1999.

[6] T. D. Breitzman, R. P. Lipton and E. V. Iarve, "Local field assessment inside multiscale composite architectures," *SIAM Journal on Multiscale Modeling & Simulation,* vol. 6, no. 3, pp. 937-962, 2007.

[7] E. V. Iarve, M. R. Gurvich, D. H. Mollenhauer, C. A. Rose and C. G. Dávila, "Mesh Independent Matrix Cracking and Delamination Modeling in Laminated Composites," *Int. J. Num. Meth. Eng.,* vol. 88, no. 8, pp. 749-773, 2011.

[8] M. de Berg, O. Cheong, M. van Kreveld and M. Overmars, Computational Geometry: Algorithms and Applications (3rd ed.), Springer-Verlag, 2008.

[9] P. E. Hart, N. J. Nilsson and B. Raphael, "A Formal Basis for the Heuristic Determination of Minimum Cost Paths," *IEEE Transactions on Systems Science and Cybernetics,* vol. 4, no. 2, pp. 100-107, 1968.

[10] E. W. Dijkstra, "A Note on Two Problems in Connexion with Graphs," *Numerische Masthematik,* vol. 1, pp. 269-271, 1959.

[11] A. Turon, P. P. Camanho, J. Costa and C. G. Dávila, "A Damage Model for the Simulation of Delamination in Advanced Composites Under Variable-Mode Loading," *Mechanics of Materials,* vol. 38, pp. 1072-1089, 2006.

[12] D. H. Mollenhauer, T. D. Breitzman, E. V. Iarve, K. H. Hoos, M. J. Swindeman and E. G. Zhou, "Simulation of mode-I fracture at the micro-level in polymer matrix composite laminate plies," in *Proc. of 53rd AIAA/ASME/ASCE/AHS/ASC SDM Conference*, Honolulu, 2012, Paper No. AIAA 2012-1651.

[13] N. J. Pagano, G. A. Schoeppner and F. Abrams, "Steady-state cracking and edge effects in thermo-mechanical transverse cracking of cross-ply laminates," *Composites Science and Technology,* vol. 58, pp. 1811-1825, 1998.